GEOPHYSICAL RESEARCH LETTERS, VOL. 32, L03111, doi:10.1029/2004GL021508, 2005

Formation of He^{2+} shell-like distributions downstream of the Earth's bow shock

Q. M. Lu and S. Wang

School of Earth and Space Sciences, University of Sciences and Technology of China, Hefei, China

Received 15 September 2004; revised 13 December 2004; accepted 17 January 2005; published 10 February 2005.

[1] When the incident solar wind He^{2+} and H^+ distributions cross the electrostatic potential at the shock, they are decelerated differentially due to their different charge- to-mass ratios. This differential slowing will produce a He^{2+} ring-beam distribution immediately downstream from a quasi-perpendicular shock. In this letter, we perform one-dimensional (1D) hybrid simulations and investigate the evolution of the He^{2+} ring-beam distribution in magnetized plasma. The plasma is composed of three components: H^+, He^{2+} and electrons, where H^+ has a velocity distribution with large perpendicular temperature anisotropy. It is shown that both the He^{2+} ring-beam distribution and H^+ distribution with large perpendicular temperature anisotropy can excite ion cyclotron waves with propagation direction parallel to the ambient magnetic field, and then the waves pitch-angle scatter the He^{2+} ions. However, only the ion cyclotron waves excited by the He^{2+} ring-beam distribution can transform He^{2+} into shell-like distribution. The results can explain the He^{2+} shell-like distributions downstream of the Earth's bow shock, which have already been observed with the AMPTE/CCE and ISEE spacecraft. **Citation:** Lu, Q. M., and S. Wang (2005), Formation of He^{2+} shell-like distributions downstream of the Earth's bow shock, *Geophys. Res. Lett.*, *32*, L03111, doi:10.1029/2004GL021508.

1. Introduction

[2] The bow shock is formed upstream from the Earth in order to slow the incoming solar wind plasma from supersonic to subsonic and to deflect this plasma around the magnetospheric obstacle. Although the structures of this collisionless shock and the evolution of the solar wind proton distributions across the bow shock have been extensively studied in recent years by analyzers on orbiting spacecraft and by theoretical investigations [*Burgess*, 1989b; *Schwartz et al.*, 1992; *Matsukiyo and Scholer*, 2003; *Lembege et al.*, 2004], the behavior of the solar wind minor ions was studied only by a few papers [*Shelley et al.*, 1976; *Peterson et al.*, 1979; *Ogilvie et al.*, 1982; *Winske et al.*, 1985; *Burgess*, 1989a; *Motschmann et al.*, 1991; *Motschmann and Glassmeier*, 1993; *Fuselier et al.*, 1988, 1991; *McKean et al.*, 1996; *Fuselier and Schmidt*, 1997].

[3] These minor ions in the solar wind usually have very low concentrations relative to H^+. Among these minor ion species, He^{2+} is the most common solar wind ion after H^+, which constitutes typically about 4% of the total solar wind ion density in number. Bow shock theory and simulations have shown that these minor ions don't adversely affect the shock structures and can be treated approximately as test particles at the shock. *Fuselier and Schmidt* [1997] proposed a simple He^{2+} injection model, in which the bow shock is considered as an infinitely thin electrostatic potential at the shock. They ignore any effects that might arise because the velocities of the distributions change over a finite shock thickness. The electrostatic potential at the shock causes H^+ slow more than He^{2+} because H^+ has larger charge-to-mass ratio, and thus in the downstream region there is a different velocity between H^+ and He^{2+} if they are assumed to have the same bulk velocity in the solar wind. He^{2+} is "injected" with its velocity relative to H^+ into the immediate downstream region, which produces a He^{2+} ring-beam distribution immediately downstream from a quasi-perpendicular shock.

[4] The observations of He^{2+} and other minor ions in the downstream of the shock have shown that they have shell-like distributions. *Peterson et al.* [1979] found that the He^{2+} distribution have a flat top at low velocities in the downstream of the shock, which can be interpreted as an unresolved or filled He^{2+} shell. *Fuselier et al.* [1988, 1997] reported He^{2+} and O^{6+} shell-like distributions downstream from the bow shock and a larger radius of O^{6+} shell than that of He^{2+}. Hybrid simulations also show that He^{2+} has shell-like distributions in the downstream of quasi-perpendicular and quasi-parallel shocks [*Motschmann and Glassmeier*, 1993; *Trattner and Scholar*, 1993]. In this paper, with a 1D hybrid simulation code, we investigate the evolution of the He^{2+} ring-beam distribution in the downstream of quasi-perpendicular shocks.

2. Simulation Model

[5] A one-dimensional (1D) hybrid code [*Winske et al.*, 1985] is employed in our simulations. The plasma consists of two ion components (H^+ and He^{2+}) and the electron component. He^{2+} contains 4% of total ion number density. Initially, the electron fluid bears zero average flow speed, and H^+ satisfies bi-Maxwellian velocity distribution with $T_{\perp p}/T_{\parallel p} > 1$ (the subscripts $\parallel$ and $\perp$ denote the directions parallel and perpendicular to the ambient magnetic field). He^{2+} is assumed to satisfy ring-beam distribution and its initial temperature is four times of the parallel temperature of H^+, which is consistent with the observations in the solar wind [*Feldman et al.*, 1996; *Gary et al.*, 2001]. According to the He^{2+} injection model of *Fuselier and Schmidt* [1997], the shock can be modeled as an effective potential. Due to their different charge to mass ratios, the shock slows H^+ more than He^{2+}, which results in a relative velocity between H^+ and He^{2+} just downstream of the collisioness shock. The

0094-8276/05/2004GL021508$05.00

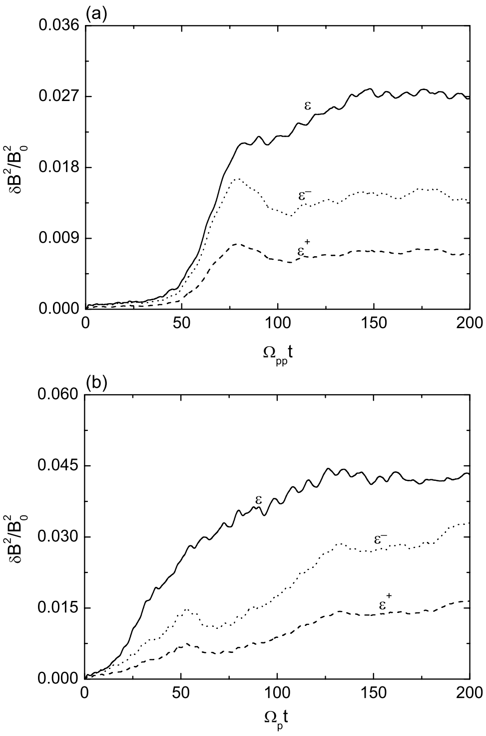

Figure 1. The time history of $\varepsilon = \delta B^2/B_0^2(\delta B^2 = B_y^2 + B_z^2)$, the total magnetic field energy, ε^+, the magnetic field energy of positive helicity, ε^-, the magnetic field energy of negative helicity. (a) $T_{\perp p}/T_{\parallel p} = 1.5$, (b) $T_{\perp p}/T_{\parallel p} = 2.7$.

difference of their velocities is called the injection velocity. By considering a special case, we can obtain an estimation of the magnitude of the injection velocity. For a supercritical, high Mach number, nearly perpendicular shock, the injection speed is about $0.4|\mathbf{V}_{sw}|$ ($|\mathbf{V}_{sw}|$ is the amplitude of the solar wind speed) [*Fuselier and Schmidt*, 1997]. In our simulation we choose the He^{2+} injection speed as $2.2V_A$ (V_A is the local Alfvén speed) and the injection angle (the angle between the injection speed and downstream magnetic field) $\alpha = 80°$.

[6] The simulations are performed in the center-of-mass frame, and periodic boundary conditions are used. The background magnetic field is assumed to be $\mathbf{B}_0 = B_0\hat{\mathbf{x}}$. We use 128 grid cells with 800 particles per cell for each ion component. The grid size is $\Delta x = 1.0c/\omega_{pp}$, where c/ω_{pp} is the ion inertial length. The time step is taken to be $\Omega_p t = 0.04$, where Ω_p is the proton gyro frequency. The proton plasma $\beta_p = 0.5$, where β_p is the ratio of kinetic pressure of the protons to magnetic pressure.

3. Simulation Results

[7] Both the He^{2+} ring-beam distribution and H^+ distribution with large perpendicular temperature anisotropy can excite electromagnetic waves. According to the method developed by *Terasawa et al.* [1986], we can separate the wave fluctuations into positive and negative helical parts. For positive helicity, forward propagating waves will be right-hand polarized (magnetosonic waves), whereas waves propagating backward will be left-hand polarized (Alfvén/ion cyclotron waves). Similarly, forward propagating waves with negative helicity will be left-hand polarized (Alfvén/ion cyclotron waves), whereas the backward propagating ones will be right-hand polarized (magnetosonic waves) [*Araneda et al.*, 2002]. In our simulations, we choose two different values for the H^+ temperature anisotropy: (a) $T_{\perp p}/T_{\parallel p} = 1.5$, (b) $T_{\perp p}/T_{\parallel p} = 2.7$. In case (a), the dominated waves are excited by the He^{2+} ring-beam distribution. In case (b), the dominated waves are excited by the large H^+ perpendicular temperature anisotropy. Figure 1 shows the time history of $\varepsilon = \delta B^2/B_0^2$ ($\delta B^2 = \underline{B_y^2} + B_z^2$), the total fluctuating magnetic field energy, ε^+, the fluctuating magnetic field energy of positive helicity, ε^-, the fluctuating magnetic field energy of negative helicity, for case (a) and (b). Both the positive and negative helical waves can be excited, and the negative helical waves have larger amplitudes than that of positive helical waves. For case (a), the waves begin to be excited at $\Omega_p t \sim 50$, and saturate at $\Omega_p t \sim 80$. For case (b), the waves begin to be excited at $\Omega_p t \sim 20$, and saturate at $\Omega_p t \sim 120$. At the quasi-equilibrium stage, the average amplitudes of waves are about $\delta B/B_0 \approx 0.16$ and 0.21 for case (a) and case (b) respectively.

[8] Detailed analysis shows that both the positive and negative helical waves are left-hand polarized. The positive helical waves propagate backward while the negative helical waves propagate forward. Therefore both the positive and negative helical waves are ion cyclotron waves. Actually the waves excited in case (a) are similar to the waves excited by He^{2+} bi-Maxwellian distributions with large perpendicular temperature anisotropy [*Gary et al.*, 1994]. In Figure 2 we

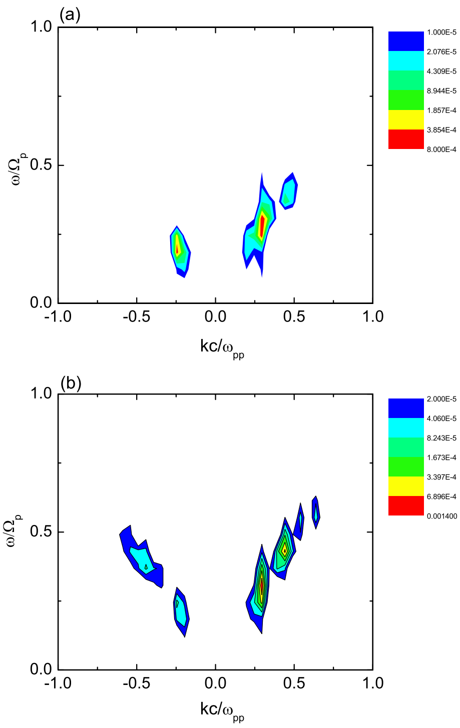

Figure 2. The characteristics of ω–k diagram obtained by Fourier transformation of the magnetic fields in the y direction from $\Omega_p t = 0$ to $\Omega_p t = 102.4$, the negative k means that the waves propagate backward whereas the waves with positive k propagate forward. (a) $T_{\perp p}/T_{\parallel p} = 1.5$, (b) $T_{\perp p}/T_{\parallel p} = 2.7$.

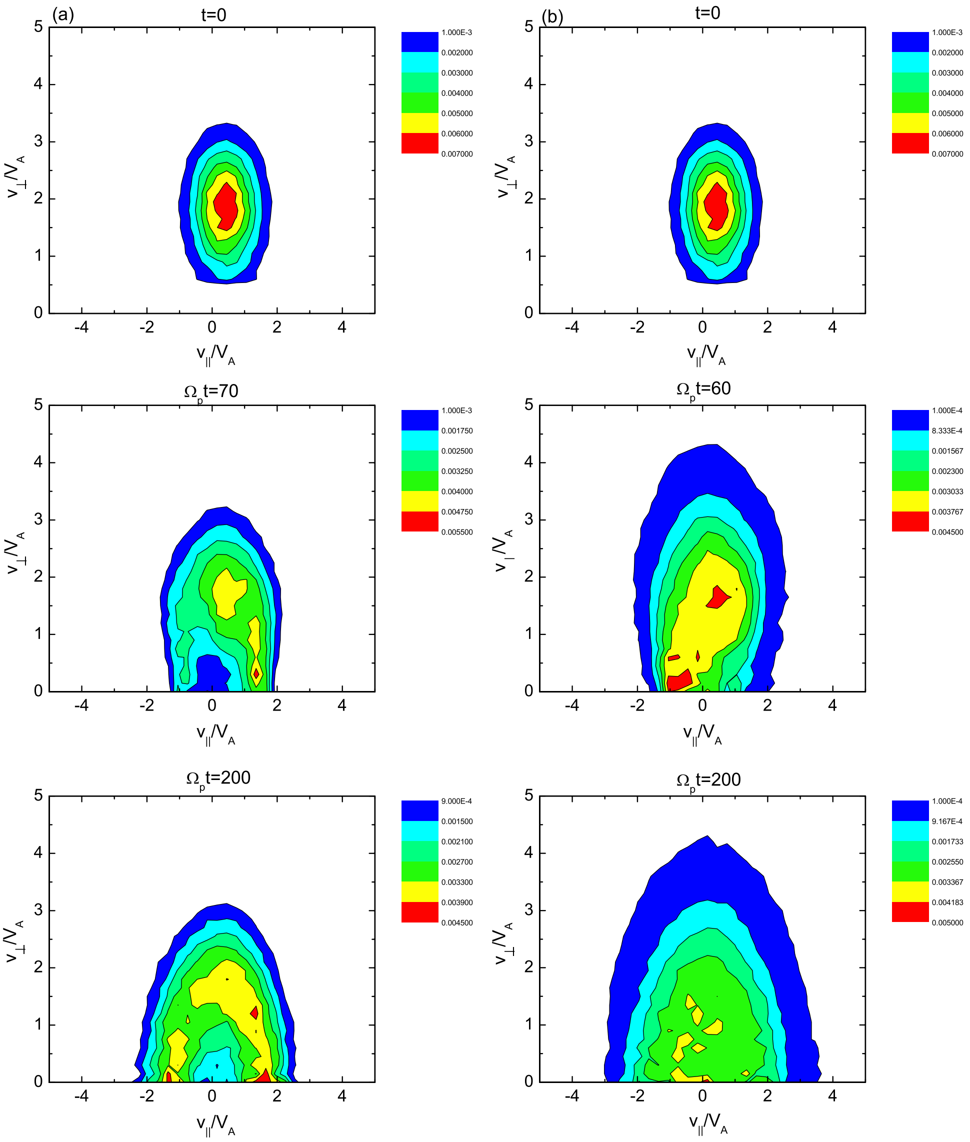

Figure 3. The He^{2+} velocity distributions at different times. In the figure, $v_{\|} = v_x$ and $v_{\perp} = \sqrt{v_y^2 + v_z^2}$. (a) $T_{\perp p}/T_{\| p} = 1.5$, (b) $T_{\perp p}/T_{\| p} = 2.7$.

show the characteristics of ω–k diagram obtained by Fourier transformation of the fluctuating magnetic fields B_y^+ and B_y^- from $\Omega_p t = 0.0$ to $\Omega_p t = 102.4$. In case (a), the frequencies of the waves excited by the He^{2+} ring-beam distributions is below the He^{2+} cyclotron frequency, while in case (b) the frequencies of the waves excited by the H^+ large perpendicular temperature anisotropy can exceed the He^{2+} cyclotron frequency.

[9] The excited waves can pitch-angle scatter He^{2+} and transform its velocity distribution. Figure 3 describes the evolution of the He^{2+} velocity distribution $f(v_{\|}, v_{\perp})$ at different times for case (a) and (b). Initially, the He^{2+} ions concentrate near $v_{\|} = 0.38V_A$ and $v_{\perp} = 2.17V_A$, which is a ring-beam distribution with the radius $2.2V_A$. For case (a), with the excitation of the ion cyclotron waves, He^{2+} is pitch-angle scattered by the ion cyclotron waves. The radius of the ring-beam decreases, and at the same time the velocities in the direction parallel to the ambient magnetic field increases. At $\Omega_p t \sim 100$, a shell-like velocity distribution of He^{2+} is formed with the radius about $1.5V_A$, which seems to last very long time. Even at the end stage of our simulations it still persists. However for case (b), at the quasi-equilibrium stage the He^{2+} distribution approximately satisfies a Maxwellian function, not a shell-like distribution.

4. Summary and Discussions

[10] Due to their different charge to mass ratios, the incident solar wind H^+ and He^{2+} slow differentially across the boundary of the shock, which can form a He^{2+} ring-beam distribution in the downstream of the quasiperpendicular collisionless shock. In this letter, with a 1D hybrid simulation code we investigated the evolution of the He^{2+} ring-beam distributions in magnetized plasma where the H^+ component has a large perpendicular temperature anisotropy. The results demonstrate that both the He^{2+} ring-beam distribution and H^+ distribution with large perpendicular temperature anisotropy can excite the left-hand

polarized ion cyclotron waves propagating parallel and antiparallel to the ambient magnetic field. However, it is the ion cyclotron waves excited by the He^{2+} ring-beam distribution that can pitch-angle scatter He^{2+} into shell-like velocity distribution with the radius a little smaller than that of its initial ring-beam distribution.

[11] Observations with AMPTE/CCE and ISEE spacecraft have shown that He^{2+} have shell-like velocity distributions downstream of the Earth's bow shock [*Fuselier et al.*, 1988; *Fuselier and Schmidt*, 1997], and computer simulations have also found the He^{2+} shell-like distributions in this area [*Motschmann and Glassmeier*, 1993]. It is generally accepted that the electromagnetic waves downstream of shock scatter the He^{2+} from ring-beam distributions to shell-like distributions. However, it is still unclear which kind of waves scatters He^{2+} into shell-like distribution. Our simulation results suggest that He^{2+} shell-like velocity distributions are formed by the waves excited by its own ring-beam distributions. In our study, we ignore the thickness of the shocks and perform the 1D hybrid simulation in the downstream frame which moves with the average speed of the protons. If the shock thickness is considered, the formation process of the He^{2+} shell-like distributions could be more complicated than what we have described. The ring-beam and shell-like distributions of He^{2+} may be occur simultaneous in the downstream of the shock and form a nongyrotropic ring distribution in the downstream frame as pointed by *McKean et al.* [1995b]. The waves and particle evolution downstream of quasi-perpendicular shocks have also been studied by *McKean et al.* [1995a, 1996] with a 2D hybrid simulation, and the shock is also included in their model. They found that the large H^+ temperature anisotropy behind the shock overshoot can excite the proton cyclotron waves, which are then convected to downstream with the average speed of the protons. If it is correct, a 1-D simulation is not appropriate to describe the excitation and propagation of the proton cyclotron waves downstream of a shock. However, in their study the He^{2+} are heated in the direction perpendicular to the ambient magnetic field through absorption of proton cyclotron waves and become gyrotropic. The dynamics of He^{2+} is controlled by the proton cyclotron waves, which is similar to our case (b). When the evolution of the He^{2+} velocity distribution is dominated by the waves excited by the He^{2+} ring-beam distribution (like our case (a)), a 1-D simulation model as presented in this letter can describe the evolution of He^{2+} velocity distributions no matter how the proton cyclotron waves are excited.

[12] **Acknowledgment.** This research was supported by the National Science Foundation of China (NSFC) under Grants 40304012 and 40336052 and Chinese Academy of Sciences Grant KZCX2-SW-136.

References

Araneda, J. A., A. F. Viñas, and H. F. Astudillo (2002), Proton core temperature effects on the relative drift and anisotropy evolution of the ion beam instability in the fast solar wind, *J. Geophys. Res.*, *107*(A12), 1453, doi:10.1029/2002JA009337.

Burgess, D. (1989a), Alpha particles in field-aligned beams upstream of the bow shock: Simulations, *Geophys. Res. Lett.*, *16*, 163–166.

Burgess, D. (1989b), Cyclic behavior at quasi-parallel collisionless shocks, *Geophys. Res. Lett.*, *16*, 345–348.

Feldman, W. C., B. L. Barraclough, J. L. Phillips, and Y. M. Wang (1996), Constraints on high-speed solar wind structures near its coronal base: A Ulysses perspective, *Astron. Astrophys.*, *316*, 355–367.

Fuselier, S. A., and W. K. H. Schmidt (1997), Solar wind He^{2+} ring-beam distributions downstream from Earth's bow shock, *J. Geophys. Res.*, *102*, 11,273–11,280.

Fuselier, S. A., E. G. Shelley, and D. M. Klumpar (1988), AMPTE/CCE observations of the shell-like He^{2+} and O^{6+} distributions in the magnetosheath, *Geophys. Res. Lett.*, *15*, 1333–1336.

Fuselier, S. A., O. W. Lennartsson, M. F. Thomsen, and C. T. Russell (1991), He^{2+} heating at a quasi-parallel shock, *J. Geophys. Res.*, *96*, 9805–9810.

Gary, S. P., P. D. Convery, R. E. Denton, S. A. Fuselier, and B. J. Anderson (1994), Proton and helium cyclotron anisotropy instability thresholds in the magnetosheath, *J. Geophys. Res.*, *99*, 5915–5921.

Gary, S. P., B. E. Goldstein, and J. T. Steinberg (2001), Helium ion acceleration and heating by Alfvén/cyclotron fluctuations in the solar wind, *J. Geophys. Res.*, *106*, 24,955–24,963.

Lembege, B., et al. (2004), Selected problems in collisionless-shock physics, *Space Sci. Rev.*, *110*, 161–226.

Matsukiyo, S., and M. Scholer (2003), Modified two-stream instability in the foot of high Mach number quasi-perpendicular shocks, *J. Geophys. Res.*, *108*(A12), 1459, doi:10.1029/2003JA010080.

McKean, M. E., N. Omidi, and D. Varban (1995a), Wave and ion evolution downstream of quasi-perpendicular bow shocks, *J. Geophys. Res.*, *100*, 3427–3437.

McKean, M. E., N. Omidi, D. Krauss-Varban, and H. Karimabadi (1995b), Wave and particle evolution downstream of quasi-perpendicular shocks, *Adv. Space Res.*, *15*, 319–322.

McKean, M. E., N. Omidi, and D. Krauss-Varban (1996), Magnetosheath dynamics downstream of low Mach number shocks, *J. Geophys. Res.*, *101*, 20,013–20,022.

Motschmann, U., and K. H. Glassmeier (1993), Simulation of heavy ion ring and shell distributions downstream of the bow shock, *Geophys. Res. Lett.*, *20*, 987–990.

Motschmann, U., K. Sauer, T. Roatsch, and J. F. Mckenzie (1991), Subcritical multiple-ion shocks, *J. Geophys. Res.*, *96*, 13,841–13,848.

Ogilvie, K. W., M. A. Coplan, and R. D. Zwickl (1982), Helium, hydrogen, and oxygen velocities observed on ISEE 3, *J. Geophys. Res.*, *87*, 7363–7369.

Peterson, W. K., E. G. Shelley, R. D. Sharp, R. G. Johnson, J. Geiss, and H. Rosenbauer (1979), H^+ and He^{2+} in the dawnside magnetosheath, *Geophys. Res. Lett.*, *6*, 667–670.

Schwartz, S. J., D. Burgess, W. D. Wilkinson, R. L. Kissel, M. Dunlop, and H. Luhr (1992), Observations of short large-amplitude magnetic structures at a quasi-parallel shocks, *J. Geophys. Res.*, *97*, 4209–4223.

Shelley, E. G., R. D. Sharp, and R. G. Johnson (1976), He^{2+} and H^+ flux measurement in the dayside cusp: Estimates of convection electric field, *J. Geophys. Res.*, *81*, 2363–2370.

Terasawa, T., M. Hoshino, J. Sakai, and T. Hada (1986), Decay instability of finite-amplitude circularly polarized Alfven waves: A numerical simulation of stimulated Brillouin scattering, *J. Geophys. Res.*, *91*, 4171–4181.

Trattner, K. J., and M. Scholar (1993), Distribution and thermalization of protons and alpha particles at collisionless quasi-parallel shocks, *Ann. Geophys.*, *11*, 774–788.

Winske, D. (1985), Hybird simulation codes with applications to shocks and upstream waves, *Space Sci. Rev.*, *42*, 53–66.

Winske, D., C. S. Wu, Y. Y. Li, Z. Z. Mou, and S. Y. Gou (1985), Coupling of newborn ions to the solar wind by electromagnetic instabilities and their interaction with the bow shock, *J. Geophys. Res.*, *90*, 2713–2726.

Q. M. Lu and S. Wang, School of Earth and Space Sciences, University of Sciences and Technology of China, Hefei, Anhui 230026, China. (qmlu@ustc.edu.cn)